

Quantum Repeaters based on Deterministic Storage of a Single Photon in distant Atomic Ensembles

D.Aghamalyan,¹ and Yu.Malakyan^{1,2*}

¹ *Institute for Physical Research, Armenian National Academy of Sciences, Ashtarak-2, 0203, Armenia and*

² *Centre of Strong Field Physics, Yerevan State University, 1 A.Manukian St., Yerevan, 0025, Armenia*

(Dated: October 13, 2011)

Quantum repeaters hold the promise to prevent the photon losses in communication channels. Most recently, the serious efforts have been applied to achieve scalable distribution of entanglement over long distances. However, the probabilistic nature of entanglement generation and realistic quantum memory storage times make the implementation of quantum repeaters an outstanding experimental challenge. We propose a quantum repeater protocol based on the deterministic storage of a single photon in atomic ensembles confined in distant high-finesse cavities and show that this system is capable of distributing the entanglement over long distances with a much higher rate as compared to previous protocols, thereby alleviating the limitations on the quantum memory lifetime by several orders of magnitude. Our scheme is robust with respect to phase fluctuations in the quantum channel, while the fidelity imperfection is fixed and negligibly small at each step of entanglement swapping.

PACS numbers: 03.67.Hk, 03.67.Bg, 42.50.Pq

I. INTRODUCTION

Distribution of entanglement between distant matter nodes of quantum networks is a challenging task because of the exponential loss of photons in communication channels. One way to cover large distances is using quantum repeater systems [1], which split the quantum communication line into small segments and combine local atomic memories for photons with entanglement swapping to extend the entanglement generated between pairs of neighboring memory elements over the entire communication link length. Currently, a number of experiments toward realization of scalable quantum repeater systems have been successfully accomplished [2–5] on the basis of the well-known Duan, Lukin, Cirac and Zoller (DLCZ) protocol [6], where it is proposed at first to generate and store entanglement between two atomic ensembles and then to connect two pairs of entangled ensembles. As an initial step, heralded entanglement between two remotely located atomic ensembles is established by detecting a single Stokes photon emitted indistinguishably from either of the two ensembles via spontaneous Raman process resulting in the creation and storage of collective spin excitation in atoms. This has been convincingly demonstrated in the experiments mentioned above. However, the entanglement connection between two pairs of entangled ensembles, which requires controllable conversion of stored atomic excitations into anti-Stokes photons followed by their detection in the same way as the Stokes photons, was faced with serious difficulties [5]. The main reason is the probabilistic nature of the DLCZ scheme based on the key requirement of low probability for Stokes-photon emission that is needed to

avoid contamination of the entangled state by processes involving more than one atomic excitation. As a result, the entanglement creation is achieved only after many unsuccessful attempts that severely limit the efficiency of entanglement swapping even under ideal conditions of reconversion and detection of anti-Stokes photons. To overcome this limitation new schemes for improvements of the DLCZ protocol have recently been proposed [7–11], promising an exciting possibility for robust and efficient entanglement generation. However, the predicted times for overall entanglement distribution at large distances are still very long as compared to realistic quantum memory storage times.

In this paper we propose a quantum repeater protocol based on a deterministic storage of single photons in remote atomic ensembles, thus removing the inherent drawback of the probabilistic DLCZ protocol. We show that our scheme is able to generate a single cavity-mode Stokes photon with near-unit probability that provides very fast and robust entanglement swapping over large distances. This advance is made possible by introducing two key modifications over existing protocols. First,

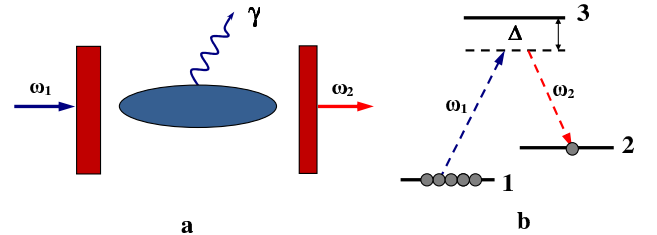


FIG. 1: (Color online)(a) Building block with atomic ensemble confined in a microcavity. γ shows fluorescence photons emitted outside the cavity. (b) Atomic level structure for emission of Stokes photon in far off-resonant Raman configuration.

*Electronic address: yumal@ipr.sci.am

we employ a single-photon excitation of the ensembles to exclude the multiatom events in the collective spin excitation and second, we use an ensemble of cold atoms strongly coupled to a high-finesse cavity field that maximally enhances the Stokes-photon generation into the cavity mode. The building block in our scheme is a Bose-Einstein condensate (BEC) of N atoms with Λ -type level structure, each of which is identically and strongly coupled to the cavity mode [Fig.1(a)]. In contrast to the thermal atoms, where the individual, position-dependent coupling for each atom to the cavity field leads to spatial inhomogeneities, in the BEC the atomic motion is almost frozen which allows one to maximize the collective coupling between the ensemble and the cavity field and to minimize position fluctuations keeping at the same time the number of atoms fixed. This has been recently realized experimentally in Refs. [12, 13].

In Fig. 1, a single-photon at the frequency ω_1 entering the one-side cavity, for example, through the left mirror, which is assumed transparent for light at this frequency, excites the atoms in the $|1\rangle \rightarrow |3\rangle$ transition and is converted via Raman scattering into the cavity-mode ω_2 photon [Fig.1(b)], which leaves the cavity through the right mirror with a transmissivity incomparably larger than that of the left mirror. The result is the storage of incident photon in the medium as a single spin excitation, which is subsequently retrieved in the anti-Stokes photon. Both processes are deterministic thanks to the multiatom collective interference effect and the cavity enhanced atom-light interaction. If all atoms are initially prepared in the ground state $|0_a\rangle = |1_1, \dots, 1_N\rangle$, then upon emitting one cavity-mode Stokes photon the atomic ensemble settles down into the symmetric state

$$|1_a\rangle = S^+|0_a\rangle = \frac{1}{\sqrt{N}} \sum_{i=1}^N |1_1, \dots, 2_i, \dots, 1_N\rangle \quad (1)$$

with one spin excitation. The collective atomic spin operator is defined as

$$S^+ = \frac{1}{\sqrt{N}} \sum_{j=1}^N \sigma_{21}^{(j)}, \quad S = (S^+)^\dagger \quad (2)$$

obeying the commutation relation $[S, S^+] \simeq 1$, following from the fact that upon interacting with the single photon, almost all the atoms are maintained in the ground state $|1\rangle$. Here $\sigma_{\alpha\beta}^{(j)} = |\alpha\rangle_j \langle\beta|$ is the atomic spin-flip operator in the basis of two ground states $|1\rangle$ and $|2\rangle$ for the j th atom. Through strongly suppressed Raman scattering into other optical modes (see below), the output state of atoms and photons can be written as

$$|\Psi_{out}\rangle = \sqrt{1-p} |0_a\rangle \otimes |1_{\omega_1}\rangle |0_{\omega_2}\rangle + \sqrt{p} |1_a\rangle \otimes |0_{\omega_1}\rangle |1_{\omega_2}\rangle \quad (3)$$

where $|0_{\omega_1}\rangle$, $|1_{\omega_1}\rangle$ and $|0_{\omega_2}\rangle$, $|1_{\omega_2}\rangle$ denote Fock states with zero and one photon of the incident and cavity fields, respectively, and p is the probability of cavity photon

emission by the atoms illuminated by the input single-photon pulse. The cavity mode is assumed to be quasi-cylindrical, while the atomic ensemble is pencil shaped and is optically thick along the cavity axis. As is shown below, this scheme is capable of producing cavity photons with probability $p \sim 1$, even if the one-photon detuning Δ is kept much larger: $\Delta \gg k, g_1, g_2$, which is desirable to make the system robust against the spontaneous loss from upper level and dephasing effects induced by other excited states. Here g_1 and g_2 are the atom-field coupling constants in the transitions $|1\rangle \rightarrow |3\rangle$ and $|2\rangle \rightarrow |3\rangle$, respectively, and k is the cavity decay rate. This significant enhancement of atom-light interaction is achieved due to the coherent coupling of different atoms to the forward-scattered Stokes photon that creates a collective atomic spin wave, which is in strong correlation with the cavity mode. Meanwhile, the field modes other than the cavity mode are weakly correlated with the collective atomic state and contribute to noise resulting in the collectively enhanced signal-to-noise ratio. This is also a basic property of the original DLCZ protocol, where, however, instead of the input single-photon pulse, a short-pulse write laser is used which gives rise to the problem of multiatom excitations. Another distinctive feature of our approach is the atom-cavity interaction in the regime of strong coupling: $g_{1,2} \gg k$, which allows one to essentially amplify the Stokes-photon generation.

The procedure for entanglement creation between the remote locations BB1 and BB2 in Fig.2 requires that either of the two atomic ensembles is excited by the ω_1 -photon such that a single Stokes photon is emitted from two ensembles. The detection of the Stokes photon, for example in D1, projects the joint state of atomic ensembles in an entangled state having the form

$$|\Psi_{12}\rangle = \frac{1}{\sqrt{2}} (|1_a\rangle_1 |0_a\rangle_2 + \exp(i\Phi_{12}) |0_a\rangle_1 |1_a\rangle_2), \quad (4)$$

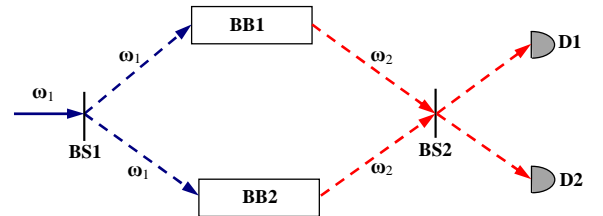


FIG. 2: (Color online) Set-up for entanglement generation between two remote ensembles, which are confined in the building blocks BB1 and BB2 shown in Fig. 1(a). A single ω_1 -photon pulse passes through a 50:50 beam-splitter (BS1) into two ensembles. The ω_2 Stokes photon emitted by either of the ensembles is mixed on a balanced beam-splitter (BS2) and detected at single photon detectors D1 and D2, thus projecting the ensembles into an entangled state with one spin excitation stored in either of the ensembles. The ω_1 photon source and detectors D1 and D2 are located in a central station between the ensembles.

where $|0_a\rangle_i$ and $|1_a\rangle_i$ are the atomic collective states for the i th ensemble ($i=1,2$) with 0 and 1 spin excitation, respectively, and $\Phi_{12} = \phi_{\omega_1}^{(1)} + \phi_{St}^{(1)} - (\phi_{\omega_1}^{(2)} + \phi_{St}^{(2)})$ stands for the difference of phases $\phi_{\omega_1,St}^{(1)}$ and $\phi_{\omega_1,St}^{(2)}$ acquired by the ω_1 - and Stokes photons on their way in the up [labeled as (1)] and down (2) sides of the channel. The state (4) is generated with efficiency increasing linearly with the Stokes-photon emission probability p , but the entanglement creation process remains probabilistic due to photon losses and various imperfections in the quantum channel, as is shown in Sec.III. Note, however, that although the suppression of photon losses in communication channels is still a serious experimental challenge, we hope that this problem will be solved by taking advantage of hollow-core photonic-crystal fibers [14]. Then, taking also into account the recent progress achieved to highly enhance the efficiencies of single-photon detection [15] and of retrieving anti-Stokes photons in cavities [16], our scheme will provide a deterministic entanglement swapping in every step with a success probability close to unity that is a fundamental difference from previous quantum repeater protocols, which even in the hypothetical case of zero losses cannot be deterministic, as their functionality relies crucially on the key requirement of low probability of Stokes-photon emission.

This paper is organized as follows. In the next section we show the ability of the presented scheme to produce cavity photons with probability $p \sim 1$. Here we find the analytic solutions for the flux and number of output Stokes photons and prove the generation of the state (3). Then, in Sec. III we calculate the entanglement distribution time taking into account different losses and imperfections in the entanglement swapping and demonstrate that our protocol is the fastest one and is robust with respect to the pathway phase fluctuations. Our conclusions are summarized in Sec. V.

II. DETERMINISTIC GENERATION OF CAVITY PHOTONS

In what follows, we use the approach employed in our earlier work [17], where the quantum theory for generation of correlated Stokes and anti-Stokes photons in the DLCZ protocol is developed. We start from the effective Hamiltonian of the system in the rotating frame

$$H = \hbar G \sqrt{N} [S^+ a_2^\dagger a_1 + H.c.] , \quad (5)$$

which is obtained by adiabatically eliminating the upper state $|3\rangle$ owing to the large one-photon detuning $\Delta = \omega_{31} - \omega_1 = \omega_{32} - \omega_2$. In Eq.(5), $a_i(a_i^\dagger)$ is the annihilation (creation) operator of i th field inside the cavity, $G = g_1 g_2 / \Delta$, and $g_i = \sqrt{2\pi\omega_i / \hbar V} \mu_{3\alpha}$, with V being the quantization volume taken equal to the interaction volume and $\mu_{\alpha\beta}$ being the dipole matrix element of the $|\alpha\rangle \rightarrow |\beta\rangle$ transition.

With the Hamiltonian (5), the Heisenberg-Langevin equations for $a_i(t)$ are given by [18]

$$\dot{a}_1(t) = -iG\sqrt{N}S a_2(t) - \frac{1}{2}(\chi + \Gamma N)a_1(t) - \sqrt{\chi}a_{1,\text{in}}(t) \quad (6)$$

$$\dot{a}_2(t) = -iG\sqrt{N}S^+ a_1(t) - \frac{1}{2}k a_2(t) - \sqrt{k}a_{2,\text{in}}(t), \quad (7)$$

where $a_{i,\text{in}}(t)$ are the operators of input fields with the properties $[a_{i,\text{in}}(t), a_{j,\text{in}}^\dagger(t')] = \delta_{ij}\delta(t-t')$, χ is the photon number damping rate for the ω_1 field, which is calculated in the free-space limit as the inverse of propagation time of the ω_1 pulse through the atomic sample: $\chi = c/L$, with L being the sample length. In Eq. (6) we have included also the losses ΓN of the ω_1 field, which originate from the emission of fluorescent photons outside the cavity [Fig. 1(a)], where $\Gamma = (g_1/\Delta)^2 \gamma_3$ [17] (γ_3 is the spontaneous decay rate of the upper level 3). However, these losses are usually very small as compared to χ , $\Gamma N \ll \chi$, and are neglected below.

For an input ω_1 pulse with duration $T \gg (\chi, k)^{-1}$, the solution of Eqs. (6) and (7) at large times takes the form

$$a_1(t) = -\frac{2}{\sqrt{\chi}} \frac{1}{1 + \eta S S^+} (a_{1,\text{in}}(t) - i\sqrt{\eta} S a_{2,\text{in}}(t)), \quad (8)$$

$$a_2(t) = -\frac{2}{\sqrt{k}} \frac{1}{1 + \eta S^+ S} (a_{2,\text{in}}(t) - i\sqrt{\eta} S^+ a_{1,\text{in}}(t)), \quad (9)$$

where $\eta = 4NG^2/(\chi k)$ represents the product of the coherent interaction rate $4NG^2/k$ with interaction time χ^{-1} .

We introduce the output photon operators $\hat{n}_{i,\text{out}}(t) = \int_{-\infty}^t a_{i,\text{out}}^\dagger(\tau) a_{i,\text{out}}(\tau) d\tau$ and find their mean values $n_{i,\text{out}}(t) = \langle \hat{n}_{i,\text{out}}(t) \rangle$ from the flux equations [19]

$$\frac{dn_{i,\text{out}}(t)}{dt} = \langle a_{i,\text{out}}^\dagger(t) a_{i,\text{out}}(t) \rangle, \quad i = 1, 2, \quad (10)$$

where the output fields $a_{i,\text{out}}(t)$ are connected with the input $a_{i,\text{in}}(t)$ and intracavity $a_i(t)$ fields by the input-output formalism [18]

$$a_{i,\text{out}}(t) - a_{i,\text{in}}(t) = \sqrt{r_i} a_i(t) \quad i = 1, 2, \quad (11)$$

with $r_{1,2} = (\chi, k)$. The mean value $\langle \hat{O} \rangle = \langle \Psi_{\text{in}} | \hat{O} | \Psi_{\text{in}} \rangle$ of any Heisenberg operator \hat{O} is calculated with the initial state $|\Psi_{\text{in}}\rangle = |0_a\rangle \otimes |1_{\omega_1}\rangle |0_{\omega_2}\rangle$. Then, using Eqs. (8), (9) and (11) and recalling that $SS^+|\Psi_{\text{in}}\rangle \simeq |\Psi_{\text{in}}\rangle$, for the vacuum input at Stokes frequency $\langle a_{2,\text{in}}^\dagger(t) a_{2,\text{in}}(t) \rangle = 0$ we readily find

$$\frac{dn_{1,\text{out}}(t)}{dt} = \frac{(1-\eta)^2}{(1+\eta)^2} |f(t)|^2 \quad (12)$$

$$\frac{dn_{2,\text{out}}(t)}{dt} = \frac{4\eta}{(1+\eta)^2} |f(t)|^2 \quad (13)$$

where the initial flux $\langle a_{1,\text{in}}^\dagger(t) a_{1,\text{in}}(t) \rangle$ of ω_1 field is expressed in terms of the pulse temporal envelope $f(t)$, given by

$$\langle 0 | a_{1,\text{in}}(t) | 1_{\omega_1} \rangle = f(t) \quad (14)$$

and normalized as $\int_{-\infty}^{\infty} |f(t)|^2 dt = 1$, indicating that the number of impinged photons is 1. Similarly, the wave functions of the output modes are determined as $\langle 0 | a_{i,\text{out}}(t) | \Psi_{\text{in}} \rangle = \Phi_i(t)$, giving for the output photon numbers

$$n_{i,\text{out}} \equiv n_{i,\text{out}}(\infty) = \int_{-\infty}^{\infty} |\Phi_i(t')|^2 dt'. \quad (15)$$

From Eqs. (12)-(14) it follows that the waveform of the emitted Stokes-photon reproduces the shape of the input ω_1 pulse up to a constant factor. Besides, the total number of photons is conserved: $n_{1,\text{out}}(\infty) + n_{2,\text{out}}(\infty) = n_{1,\text{in}} = 1$, showing the ability of the system to produce Stokes photons with probability $p = n_{2,\text{out}}/n_{1,\text{in}} = 1$, if $\eta = 1$ or

$$\frac{4NG^2}{k} = \chi. \quad (16)$$

Thus, we arrive at a quite reasonable requirement that for deterministic Stokes-photon generation the collectively enhanced Raman process should be as fast as the passage of the ω_1 pulse through the atomic sample. In this case the Stokes photon wave form (13) is identical to the input pulse shape $|f(t)|^2$. Note, that for larger values of η the conversion is not complete, $n_{1,\text{out}}(\infty) > 0$, because of, although weak, backward transformation of the Stokes photon into the ω_1 photon.

It is useful to consider numerical estimations at this point. As a sample the ^{87}Rb vapor is chosen with the ground states $5S_{1/2}(F=1)$ and $5S_{1/2}(F=2)$ and the excited state $5P_{3/2}(F'=2)$ being the atomic states 1, 2 and 3 in Fig. 1(b), respectively. For the light wavelength $\lambda \simeq 0.8\mu\text{m}$, $\gamma_3 = 2\pi \times 6$ MHz, $g_1 \sim g_2 = 10\gamma_3$, $\Delta \sim 50\gamma_3$, $k = 3\gamma_3$, and atomic trap length $L \sim 100\mu\text{m}$ we find that Eq.(14) is fulfilled with $N \sim 10^6$. At the same time the number of fluorescent photons is negligibly small: $\Gamma N/\chi \ll 1$. All these parameters appear to be within experimental reach, including the deterministic sources of initial narrow-band single-photon pulses with a duration of several microseconds [20–24] and BEC with $\sim 10^6$ atoms in the QED cavity [12, 13].

In the Schrodinger picture, we obtain the output state $|\psi_{\text{out}}\rangle$ of the system as the eigenstate of total photon number operator

$$(\hat{n}_{1,\text{out}}(\infty) + \hat{n}_{2,\text{out}}(\infty)) |\psi_{\text{out}}\rangle = |\psi_{\text{out}}\rangle \quad (17)$$

where the output modes are described by known wave functions $\Phi_i(t)$. To construct this state, we introduce the operators of creation of single-photon wave packets

at frequencies ω_i associated with mode functions $\Phi_i(t)$ as [25]

$$\hat{c}_i^\dagger = \frac{1}{\sqrt{n_{i,\text{out}}}} \int_{-\infty}^{\infty} dt \Phi_i(t) a_{i,\text{out}}^\dagger(t) \quad (18)$$

These operators create single-photon states in the usual way by acting on the field vacuum $|0_f\rangle = \prod_i |0_{\omega_i}\rangle$

$$\hat{c}_i^\dagger |0_f\rangle = |1_{\omega_i}\rangle |0_{\omega_j}\rangle, \quad i, j = 1, 2; \quad i \neq j \quad (19)$$

where Eq. (15) has been used. In the right-hand side of Eq. (19) the field vacuum is reduced to $|0_f\rangle = |0_{\omega_1}\rangle |0_{\omega_2}\rangle$, since other modes are not occupied by the photons and, hence, are not taken into account during the measurements. The operators c_i satisfy the standard boson commutation relations,

$$[\hat{c}_i, \hat{c}_j^\dagger] = \delta_{ij}, \quad (20)$$

that follow from the commutation relations of the output fields $\langle [a_{i,\text{out}}(t), a_{j,\text{out}}^\dagger(t')] \rangle = \delta_{ij} \delta(t-t')$, which are simply found using Eqs. (8), (9) and (11). From this, we easily find the output state

$$|\Psi_{\text{out}}\rangle = \sqrt{n_{1,\text{out}}} |0_a\rangle \otimes c_1^\dagger |0_f\rangle + \sqrt{n_{2,\text{out}}} |1_a\rangle \otimes c_2^\dagger |0_f\rangle, \quad (21)$$

which is exactly the state (3). In the general case of $n_{1,2,\text{out}} \neq 0$, the system produces a photonic qubit, i.e., a single-photon state entangled in two distinct frequency modes with wave functions $\Phi_1(t)$ and $\Phi_2(t)$. The pure output state $|\psi_{\text{out}}\rangle = |1_a\rangle \otimes |0_{\omega_1}\rangle |1_{\omega_2}\rangle$ consisting of a single Stokes photon and one spin excitation in the atomic ensemble is obtained in the limit of complete conversion of input ω_1 mode into the Stokes photon under the condition (16). From Eq. (21) we immediately find the number of spin-wave excitations $N_{\text{sp}} = \langle S^+ S \rangle = n_{2,\text{out}}$. This result is followed also from the comparison of Heisenberg equations for \hat{N}_{sp} and $\hat{n}_{2,\text{out}}$, if the relaxations are negligibly small, as is the case here.

III. ENTANGLEMENT DISTRIBUTION RATE

The time T_{tot} required for entanglement distribution over a distance L can be calculated by the same methods that are used for the original DLCZ protocol [6, 11]. The main difference between the two schemes occurs only in the entanglement preparation stage, so that, by separating out the success probability P_0 of entanglement generation between two atomic ensembles in the elementary link, the general formula (13) for the distribution time obtained in Ref.[11] can be rewritten as

$$T_{\text{tot}} = T_{\text{tot,DLCZ}} \frac{P_{0,\text{DLCZ}}}{P_0}. \quad (22)$$

Here we have taken into account that in the entanglement swapping the anti-Stokes photon being far from the resonance with the cavity is generated as in the free space and, hence, the cavity has no effect on the excitation transfer from the collective atomic mode to the optical mode. The dominant noise that limits the success probability P_0 is the photon losses, which include the transmission channel losses and the inefficiency of single-photon detectors. Correspondingly, $P_0 = p\eta_d\eta_t$ is defined as the product of quantum-mechanical probability p of Stokes-photon emission by the photon detection efficiency η_d and the transmission efficiency $\eta_t = \exp(-\frac{L_0}{L_{\text{att}}})$, where L_0 is the distance between the atomic ensembles (or the length of the elementary link) in Fig. 2 and L_{att} is the communication channel attenuation length. Compared to the DLCZ scheme, the transmission efficiency is quadratically smaller: $\eta_t = \eta_{t,\text{DLCZ}}^2$, since in our case we have to include the transmission losses both for ω_1 photon propagating from the source to the atomic ensembles and for the Stokes photon propagating back to the detectors placed in the central station. This leads to a notable increase of T_{tot} , which, however, is compensated by another effect. Indeed, the deterministic generation of the Stokes photon relaxes the limitations for the quantum memory lifetime, thus allowing one to enhance the memory efficiency η_m . Since $T_{\text{tot,DLCZ}}$ in Eq.(22) is inverse proportional to the success probabilities at each level of entanglement connection or to η_m^{n+2} [11], where $L_0 = \frac{L}{2^n}$, then by properly choosing the parameters one can ensure that the two effects of lowering η_t and increasing of η_m cancel each other in T_{tot} for arbitrary communication length L . As such, taking into account that usually $p_{\text{DLCZ}} < 0.01$, we find that in the present scheme with $p \sim 1$ the entanglement distribution rate T_{tot}^{-1} increases at least by 2 orders of magnitude as compared to that of the original DLCZ protocol. For example, for the parameters used in Fig. 18 of Ref. [11] $L_{\text{att}} \sim 22\text{km}$ (this corresponds to a fiber attenuation of 0.2 dB/km for telecom wavelength photons), $\eta_d \sim 1$ [15], and $n = 4$, and for $\eta_m \sim 1$, the total time needed in our scheme for distributing a single entangled pair over the distance $L = 1000\text{ km}$ is only 10 s, thus making our protocol the fastest one and comparable with the multimode-memory-based protocol of Ref. [26]. It is worth noting that, while achieving much faster performance, our proposal has an advantage in robustness. In the probabilistic protocols [11], the errors which reduce the fidelity of the distributed state are mainly caused by the event when more than one atom is excited into the collective spin wave, whereas only one Stokes photon is detected. This process is forbidden in our scheme, and, hence, the fidelity imperfection is fixed and negligibly small during all the time of entanglement distribution. Furthermore, our scheme is much more robust with respect to phase fluctuations in the fibers. To show this let us remind that the phase Φ_{12} in Eq.(4) is sensitive to path-length fluctuations leading to phase instability of entanglement connection between the two pairs of entangled ensembles [6, 11]. Suppose that two

pairs of atomic ensembles (1,2) and (3,4) are prepared in independent entangled states like the state (4) with the phases Φ_{12} and Φ_{34} , respectively, and that the connection between the pairs performed by the standard procedure [6, 11] projects their state into a maximally entangled state between the four atomic ensembles,

$$|\Psi_{12,34}\rangle = \frac{1}{\sqrt{2}}(|1_a\rangle_1|1_a\rangle_4 + \exp(i\delta\Phi)|1_a\rangle_3|1_a\rangle_2), \quad (23)$$

where $\delta\Phi = \Phi_{12} - \Phi_{34}$ is the relative phase between the two entangled pairs. Since the entanglement generation process is probabilistic and, hence it is established in the pairs at different time moments although the entanglement preparation begins in the two pairs simultaneously, the phases Φ_{12} and Φ_{34} are different due to path length fluctuations during this time interval. The mean value of the latter can be estimated as the duration of entanglement generation between two atomic ensembles in the elementary link: $\tau \sim L_0/(cP_0)$. For $L_0 \sim 60\text{km}$, $p = 1$ and for the rest parameters given above we have $\tau \sim 0.004\text{s}$. This means that the Stokes-photon coming time must be controlled over this averaged time with accuracy of the order of $\omega^{-1} \sim 10^{-15}\text{s}$ ($\omega \sim \omega_1 \sim \omega_2$), corresponding to $\delta\Phi < 1$, which is achievable for current technologies [27]. Note that in the DLCZ protocol $\tau \sim 1\text{s}$ for the same parameters that makes the phase stabilization hardly feasible. A much more favorable situation occurs if the both the entanglement generation and the swapping are done via two-photon detection similar to the protocol proposed in Ref. [28], in contrast to the DLCZ protocol based on a single-photon detection. As has been shown in Ref. [28], in this case the propagation phases that two photons acquire only lead to a multiplicative factor to the pair entangled state. Moreover, if in Ref. [28] the total state-function of two entangled pairs, apart from the entangled part, contains also the contribution from multiatom excitations that deteriorates the final-state fidelity, in our case the photonic part of the state (3) for $p = 1$ has no vacuum and two- or more photon components; hence the two pairs are in a pure maximally entangled state, thus making the long-distance phase stabilization unnecessary.

IV. CONCLUSIONS

Summarizing, we have described a quantum repeater protocol that uses an input single-photon pulse instead of a write laser in the original DLCZ scheme, thus avoiding the problem of multiple atomic spin excitations. Also a high-finesse cavity is employed to maximally enhance the Raman conversion of input photon into forward scattered Stokes light mode. The main advantage of this setup is that it does not constrain the probability of Stokes-photon generation, which can be made equal to unity by adjusting the system parameters. As a result, the errors, which reduce the fidelity in the conventional

DLCZ protocol, are strongly suppressed and the long-distance interferometric stability is no longer required. Our scheme enables a robust quantum repeater without long-living quantum memories, thus providing a fast communication rate. The proposed protocol can be also implemented with atoms confined inside a single-mode hollow-core photonic-crystal fiber.

Acknowledgments

This research has been conducted in the scope of the International Associated Laboratory IRMAS. We also acknowledge support from the Science Basic Foundation of the Government of the Republic of Armenia.

-
- [1] H. -J. Briegel, W.Dur, J. I. Cirac, and P. Zoller, Phys.Rev.Lett. **81**, 5932 (1998).
 - [2] D. N. Matsukevich and A. Kuzmich, Science **306**, 663 (2004).
 - [3] C. W. Chou, H. de Riedmatten, D. Felinto, S. V. Polyakov, S. J. van Enk, and H. J. Kimble, Nature (London) **438**, 828 (2005).
 - [4] C.W.Chou, J. Laurat, H. Deng, K. Choi, H. de Riedmatten, D. Felinto, and H.J. Kimble, Science **316**, 1316 (2007).
 - [5] J.Laurat, C.-W Chou, H. Deng, K. S. Choi, D. Felinto, H. de Riedmatten and H J Kimble, New J. Phys. **9**, 207 (2007).
 - [6] L. M. Duan, M. D. Lukin, J. I.Cirac, and P. Zoller, Nature (London) **414**, 413 (2001).
 - [7] N. Sangouard, C. Simon, J. Minar, H. Zbinden, H. de Riedmatten, and N. Gisin, Phys. Rev. A **76**, 050301(R)(2007).
 - [8] K. S. Choi, H. Deng, J. Laurat, and H. J. Kimble, Nature (London) **452**, 67 (2008).
 - [9] J. B. Brask, L. Jiang, A. V. Gorshkov, V. Vuletic, A. S. Sorensen, and M. D. Lukin, Phys. Rev. A **81**, 020303(R)(2010).
 - [10] C. Simon, H. de Riedmatten and M. Afzelius, Phys. Rev. A **82**, 010304(R) (2010).
 - [11] N. Sangouard, C. Simon, H. de Riedmatten, and N. Gisin, Rev. Mod. Phys. **83**, 33 (2011).
 - [12] F.Brennecke, T. Donner, S. Ritter, T. Bourdel, M. Kohl, and T.Esslinger, Nature (London) **450**, 268 (2007).
 - [13] Y. Colombe, T. Steinmetz, G. Dubois, F. Linke, D. Hunger, and J. Reichel, Nature (London) **450**, 272 (2007).
 - [14] P. St. J. Russell, J. Lightwave Technol. **24**, 4729 (2006).
 - [15] D.F.V. James and P.G. Kwiat, Phys. Rev. Lett. **89**, 183601 (2002); A. Imamoglu, ibid. **89**, 163602 (2002).
 - [16] J.Simon, H. Tanji, J. K. Thompson, and V. Vuletic, Phys. Rev. Lett. **98**, 183601 (2007).
 - [17] N. Sisakyan and Yu.Malakyan, Phys.Rev. A **72**, 043806 (2005).
 - [18] C. W. Gardiner and P. Zoller, *Quantum Noise*(Springer-Verlag, Berlin, 1999).
 - [19] K.J.Blow, R.Loudon, S.J.D.Phoenix, and T.J.Shepherd, Phys. Rev. A **42**, 4102 (1990).
 - [20] A. Kuhn, M. Hennrich, and G. Rempe, Phys.Rev.Lett. **89**, 067901 (2002).
 - [21] S. Chen, Yu-Ao Chen, T.Strassel, Z.-S. Yuan, Bo Zhao, J.Schmiedmayer, and J.-W. Pan, Phys.Rev.Lett. **97**, 173004 (2006).
 - [22] J. McKeever, A. Boca, A. D. Boozer, R. Miller, J. R. Buck, A. Kuzmich, H. J. Kimble, Science **303**, 1992 (2004).
 - [23] M. Hijkema, B. Weber, H. P. Specht, S. C. Webster, A. Kuhn, and G. Rempe, Nature Phys. **3**, 253 (2007).
 - [24] A. Gogyan, S. Guerin, H.-R. Jauslin, and Yu. Malakyan, Phys. Rev. A, **82**, 023821 (2010).
 - [25] A.Gogyan and Yu.Malakyan, Phys.Rev. A **77**, 033822 (2008).
 - [26] C.Simon, H. de Riedmatten, M. Afzelius, N. Sangouard, H. Zbinden, and N. Gisin, Phys. Rev. Lett. **98**, 190503 (2007).
 - [27] K. W. Holman, D. D. Hudson, and J. Ye, Opt. Lett. **30**, 1225 (2005).
 - [28] Z.-B. Chen, Bo Zhao, Yu-Ao Chen, J. Schmiedmayer, and J.-W. Pan, Phys.Rev. A **76**, 022329 (2007).